# PARAMETERIZATION OF MICROPHYSICAL PROCESSES IN A NON HYDROSTATIC PREDICTION MODEL

O.V. Drofa and P. Malguzzi

Institute of Atmospheric and Climate Sciences of the Italian National Research Council (ISAC-CNR),
Via Piero Gobetti, 101, I-40129, Bologna, Italy

## 1. INTRODUCTION

Due to the rapid increase of computing power, the horizontal scale explicitly resolved by regional numerical prediction models has gone beyond the limit of validity of the hydrostatic approximation. Even though some turbulent processes still need to be parameterized (like entrainment in strong updrafts), the explicit description of atmospheric moist convection is in the reach of non-hydrostatic prediction models having horizontal grid distances of the order of one kilometer. In devising such models, particular attention must be paid to the parameterization of the microphysical processes responsible for the formation of clouds and precipitation.

In this paper, following a brief highlight of the ISAC-CNR non-hydrostatic model (section 2), the parameterization of the microphysical processes are described in detail in section 3. The scheme presented here is original in many respects; in particular, the parameterization of fast processes (see section 3) takes into account the size distribution of cloud particles. The model is used to simulate well documented episodes of cumulonimbus development. Simulated and observed quantities like maximum vertical velocity and temperature fluctuations are compared. Results are discussed in the final section 4.

## 2. MODEL DESCRIPTION

The numerical model used in the present study (MOLOCH), developed at the ISAC-CNR, integrates in time the fully compressible set of equations governing the atmospheric motion. The basic dynamical variables are pressure, temperature, specific humidity, and the three dimensional velocity. The model terrain following vertical coordinate $\zeta$ is related to the geometric height $z$ according to the implicit formula:

$$\zeta = H\left(1 - e^{-\frac{z - h(1-\zeta/H)}{H}}\right) \qquad (2.1)$$

where $h$ is the orographic height and $H$ is the density scale height ($R_D\ T_0\ /\ g$) computed at the reference temperature $T_0$. Equation (2.1) transforms the semi-infinite $z$-axis into the finite interval [0, $H$]. In order to reduce the error in the computation of the pressure gradient force at higher levels, the $\zeta$-coordinate surfaces smoothly relax to horizontal ones above the orography. Numerical discretization is based on the Arakawa C-grid and on equally spaced vertical intervals. Time integration is splitted with a forward-backward scheme for horizontally propagating waves and implicit for vertically propagating sound waves. Advection terms are computed with the second order FBAS scheme (Malguzzi and Tartaglione, 1999). The physical package of MOLOCH consists in radiation, vertical diffusion, and soil water and energy budgets. No convective parameterization schemes are applied. The MOLOCH simulations can be nested in runs of the hydrostatic limited area model BOLAM.

## 3. MICROPHYSICAL PARAMETERIZATION

The microphysical scheme used in the MOLOCH model is the evolution of the methods proposed by Drofa (2003) and partly based on Marecal et al. (1993) and Rutledge and Hobbs (1983). The scheme predicts the time evolution of the specific concentration of four microphysical species: cloud water, cloud ice, precipitating liquid water (rain), and precipitating ice. Precipitating ice is formed by crystal hydrometeors having physical properties depending on temperature. Physical processes involving transformations between the atmospheric specific humidity $q_V$ and cloud species (see fig. 1) occur on a very short time scale and are therefore computed every model time step. The time evolution of hydrometeors is characterized by a longer scale and is computed over a longer time interval. Slow processes are summarized in fig. 2.

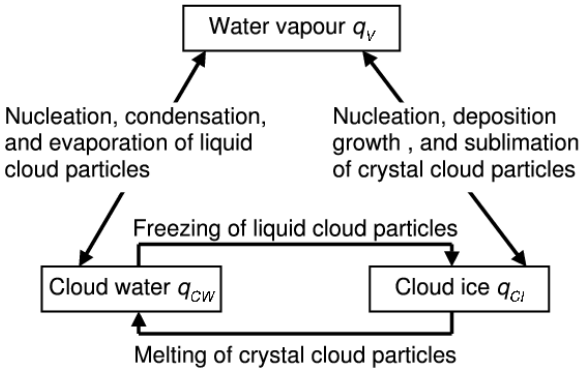


Fig.1. Schematic representation of fast processes.

All parameterized processes, apart from auto-conversion of precipitation, are based on the computation of the mass tendency of a particle of diameter $D$. The tendency of the specific concentration, say $q$, of a given microphysical specie is then obtained by the general formula:

$$\partial q/\partial t = \frac{1}{\rho_{air}} \int_0^\infty dm/dt\ N(D)\ dD \qquad (3.1)$$

where $N(D)$ is the volumetric concentration of particles per unit size $D$. For cloud particles, the gamma-distribution is used (Oblaka i Oblachnaja Atmosfera, 1989, and Volkovitzkiy et al., 1983):

$$N(D) = \frac{N_0 \beta^{\alpha+1}}{\Gamma(\alpha+1)} D^{\alpha} e^{-\beta D} \qquad (3.2)$$

where the parameter $\beta$ is determined by the integral:

$$\frac{1}{\rho_{air}} \int_0^{\infty} m(D) N(D) dD = q \,, \qquad (3.3)$$

$m(D)$ being the mass of a cloud particle, defined by:

$$m = aD^b \qquad (3.4)$$

This gives:

$$\beta = \left[ \frac{N_0 a \, \Gamma(\alpha+b+1)}{\rho_{air} \; q \; \Gamma(\alpha+1)} \right]^{\frac{1}{b}} \qquad (3.5)$$

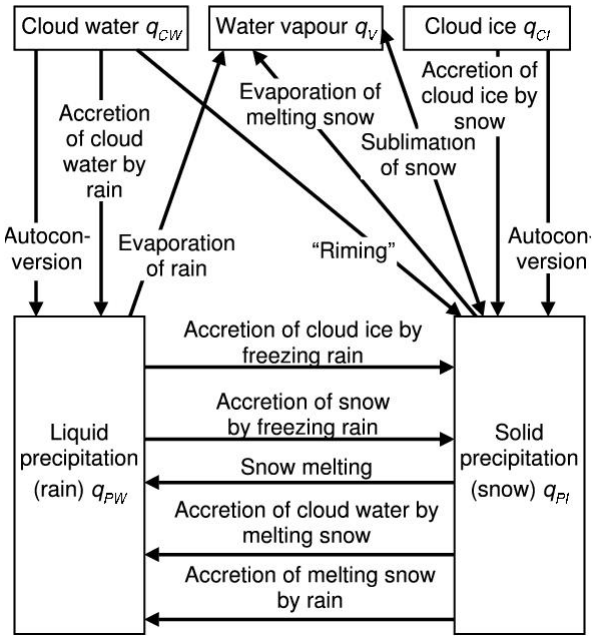


Fig.2. Schematic view of slow processes.

In the previous expressions, the parameters $N_0$, $\alpha$, $a$, and $b$ depend on the particle phase. $N_0$ holds $8.0 \cdot 10^6$ ($2.0 \cdot 10^7$) $m^{-3}$ for cloud water (cloud ice); $\alpha$ is set to 6.0 (3.0); $a = \pi \rho_W / 6$ (100.0); and $b$ =3.0 (2.5).

It is clear from (3.2) and (3.5) that the actual particle distribution depends, for a fixed $N_0$, on the specific concentration of cloud species. In particular, for small quantities of cloud water or ice, the size distribution becomes peaked towards large amounts of small diameter particles. Hence, the particle distribution has a dynamical evolution.

Similar considerations apply to the parameter-ization of processes involving precipitation. Liquid (rain) and solid (snow / ice) hydrometeors are distributed according to the Marshall-Palmer (1948) distribution:

$$N(D) = N_0 \; e^{-\lambda D} \,, \qquad (3.6)$$

where

$$\lambda = \left[ \frac{N_0 \; a \; \Gamma(b+1)}{\rho_{air} \; q} \right]^{1/(b+1)} \,. \qquad (3.7)$$

As done in the derivation of (3.5), expression (3.4) has been used here. For iced hydrometeors, the parameters $N_0$, $a$, and $b$ depend on temperature $T$ according to the following Table I (after Drofa, 2003). For liquid precipitation, the parameters $a$ and $b$ assume the same values defined for cloud water while $N_0$ is set to $8.0 \cdot 10^6$ $m^{-4}$. In the following of this section, the mass tendency associated to all of the above physical processes is given.

Table I. Values of the parameters $N_0$, $a$, $b$, $k$, and $n$ (see text) used for iced hydrometeors (Drofa, 2003).

| $T$ (° C) | $N_0$ ($m^{-4}$) | $a$ | $b$ | $k$ | $n$ |
|---|---|---|---|---|---|
| $T$ > -10 | $8 \cdot 10^6$ | 232. | 3.06 | 144. | 0.66 |
| -10 <$T$<-20 | $2 \cdot 10^7$ | 157. | 3.31 | 156. | 0.86 |
| -20<$T$ <-40 | $4 \cdot 10^7$ | 1.43 | 2.79 | 18. | 0.62 |
| $T$ < -40 | $5 \cdot 10^7$ | 0.145 | 2.59 | 7.3 | 0.55 |

Most of the microphysical processes described below are associated to heat exchanges. The corresponding temperature variations are computed from entropy conservation (its expression is given in the Appendix). The entropy of the mixture of air, ice, and water is exactly conserved by the numerical code.

### 3.1 Condensation/evaporation and sublimation

Condensation of water vapor starts over nuclei when supersaturation conditions are present. Subsequent condensation occurs over cloud droplets. Its rate is determined by assuming equilibrium between diffusive fluxes of water vapor and heat and obeys the following law, which stems out from a second order Taylor expansion of the saturation humidity with respect to temperature (Srivastava and Coen, 1992):

$$\frac{dm}{dt} = D \cdot \frac{2\pi F \left( q_V / q_{SW,SI} - 1 \right) \rho_{air}}{\dfrac{1}{q_{SW,SI} \, \chi} + \dfrac{L^v_{w,i} \; \rho_{air}}{K_A T} \left( \dfrac{L^v_{w,i}}{R_V T} - 1 \right)} \cdot$$

$$\cdot \left\{ 1 - \frac{1}{2} \left( \frac{q_V}{q_{SW,SI}} - 1 \right) \left[ \frac{\rho_{air} \left( \dfrac{L^v_{w,i}}{R_V T} - 1 \right)}{\dfrac{K_A T}{q_{SW,SI} \, \chi \, L^v_{w,i}} + \rho_{air} \left( \dfrac{L^v_{w,i}}{R_V T} - 1 \right)} \right]^2 \right. \cdot$$

$$\left. \cdot \left[ 1 + \left( 1 - 2 \frac{L^v_{w,i}}{R_V T} \right) \Big/ \left( \frac{L^v_{w,i}}{R_V T} - 1 \right)^2 \right] \right\} , \qquad (3.8)$$

where $K_A$ = 2.43·10$^{-2}$ Jm$^{-1}$K$^{-1}$s$^{-1}$ is the thermal conductivity of air; $M_W$, the molecular weight of water; $R_V$, the gas constant of water vapor; $\chi$=2.26·10$^{-5}$ m$^2$s$^{-1}$, the coefficient of molecular diffusion of vapour into air; and where the ventilation coefficient $F$ is equal to 0.8 for cloud particles and

$$F = 0.78 + 0.31\,Sc^{1/3}\left(\rho_{air} D\, u(D)/\mu\right)^{1/2} \quad (3.9)$$

for hydrometeors, $Sc$=0.6 being the Schmidt number, and $\mu$ =1.718·10$^{-5}$ kg m$^{-1}$s$^{-1}$, the dynamical molecular viscosity of air. In (3.9) $u(D)$ represents the terminal velocity of a precipitating particle that depends on pressure $P$ and is approximated by:

$$u = kD^n \left(P_0/P\right)^{0.4} \quad (3.10)$$

The parameters $k$ and $n$ hold 842.0 and 0.8, respectively, for rain. For solid hydrometeors, the values of $k$ and $n$ are given in Table I. The formula (3.8) also applies to evaporation of cloud droplets, rain, melting snow, and to sublimation of cloud and precipitating ice. In the latter case, the latent heat of sublimation $L_i^v$ and the saturation specific humidity over ice $q_{SI}$ are used.

### 3.2 Melting and freezing

When temperature is below (above) the freezing temperature of water $T_{TR}$ , freezing (melting) of cloud water (cloud and precipitating ice) occurs (see fig. 1 and 2). These processes are governed by the diffusion of heat and are parameterized according to:

$$\frac{dm}{dt} = D \cdot \frac{2\pi K_A F \left|T - T_{TR}\right|}{L_i^w} \quad (3.11)$$

where the coefficients are as in (3.8).

### 3.3 Accretion of cloud by hydrometeors

There are 5 slow processes involved (see fig. 2). Independently of temperature, accretion of cloud water by the rain drops occurs. When temperature is below $T_{TR}$, cloud ice is intercepted by precipitating ice, and sudden freezing of super cooled cloud water occurs over the surface of the precipitating ice crystals (riming). If temperature is greater than $T_{TR}$, accretion of cloud water by melting snow occurs; this process actually consists in the melting of a particle of precipitating ice caused by the heat contained in the cloud water intercepted. These four processes are governed by the following law:

$$\frac{dm}{dt} = \rho_{air}\,\frac{\pi}{4} D^2 u(D) E q_{CW,CI} \cdot \left\{C_W \left(T - T_{TR}\right)/L_i^w\right\} \quad (3.12)$$

where $E$ is the accretion coefficient, $C_W$ the specific heat of water, and where the last factor must be taken into account in the case of melting snow only. Finally, the fifth process of this group consists in the sudden freezing of precipitating water triggered by particles of cloud ice when temperature is below $T_{TR}$. This process is described by the following equation (3.13):

$$\frac{dm_{PW}}{dt} = -E\, m(D_{PW})\frac{\pi}{4} D_{PW}^2 u(D_{PW}) N_{0_{CI}} \quad (3.13)$$

The accretion coefficient holds, for the 5 processes listed above, 0.6, 0.3, 0.4, 0.4, 0.6, respectively.

### 3.4 Interaction between hydrometeors

If $T$ is less than $T_{TR}$, sudden freezing of super cooled rain occurs when a raindrop encounters a snowflake. Applying the geometric swept out concept, the mass increase of an iced hydrometeor is given by:

$$\frac{dm_{PW}}{dt} = -E\, m(D_{PW}) \left|U_{PI} - U_{PW}\right| \cdot \frac{\pi}{4}\int (D_{PW} + D_{PI})^2 N(D_{PI})\, dD_{PI} \quad (3.14)$$

where $E$=1.0 and where $U$ denotes the mass weighted mean terminal velocity of precipitation defined as

$$U = \int_0^\infty N(D)m(D)u(D)dD \Big/ \int_0^\infty N(D)m(D)dD. \quad (3.15)$$

Above freezing, a contribution to melting snow comes from the heat contained in the intercepted rain. This is computed by multiplying (3.14) by the last factor appearing in (3.12).

### 3.5 Autoconversion of precipitation

Autoconversion is the only way in which the microphysical scheme can create precipitation from clouds. This is not really a physical process, being simply a conventional redefinition of the cloud spectrum with diameter exceeding a critical value $D_0$. This is done by means of the incomplete (upper) $\Gamma$ function as follows:

$$\frac{\partial q_{CW,CI}}{\partial t} = -q_{CW,CI}\,\frac{\Gamma(\alpha + b + 1,\ \beta D_0)}{\Delta t\ \ \Gamma(\alpha + b + 1)} \quad (3.16)$$

where $\Delta t$ denotes the model time step, and where the critical diameter is set to the conventional size which separates cloud particles from rain, namely 1.0·10$^{-4}$ m for cloud water. For cloud ice, $D_0$ is 2.0·10$^{-5}$ m at $T$=$T_{TR}$ and decreases with decreasing temperature.

## 4. DISCUSSION AND CONCLUSIONS

The results obtained with the scheme described in the previous section has been tested by simulating real episodes of strong convection and cumulonimbus development.

The data used to initialize the simulations of cumulonimbus development is obtained from radio-sounding profiles of temperature and dew-point measured before strong episodes of convection. These cases have been studied in detail and are listed in Drofa (2003). To initiate convection, a saturated bubble is defined in the model initial condition in the vertical layer where near saturation conditions are observed. Model runs are performed with 250 m of horizontal and vertical resolution on a 20 by 20 km horizontal domain, and extend one hour in time. Axial symmetry around the domain center is imposed in

order to obtain well organized developments. For each simulation, the maximum value of updraft and downdraft vertical velocity, temperature fluctuations (with respect to the initial temperature profile), total water content, and simulated radar echo are computed and compared with observations. Some results are summarized in fig. 3, where observed and simulated maximum vertical velocity (triangles) and temperature anomaly (stars) are reported in a scatter plot. It can be readily seen that the model performs satisfactorily especially for very strong convective episodes. There is, nevertheless, the tendency to somewhat underestimate updrafts in relatively weak cases. However, the limited number of cases analyzed here does not allow to draw any firm conclusion.

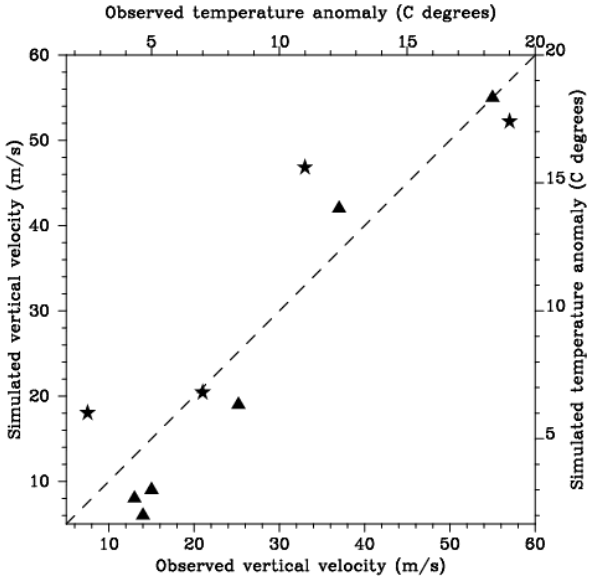


Fig3. Scatter plot of observed and simulated maximum vertical velocity in updraft (triangles) and maximum temperature fluctuations (stars). Left and bottom axis: vertical velocity in m/s. Right and top axis: temperature in $^0$C.

The above results are just preliminary ones. A more exhaustive comparison of the present scheme with more classical parameterizations, especially for what concerns microphysical variables, should be performed in order to assess the validity of the hypotheses made here. Moreover, the proposed scheme can be improved in several ways, for instance by inserting a new prognostic variable for hail. Research on these topics is under way.

## APPENDIX

The exact expression for entropy is:

$$E = C_P \log\frac{T}{T_0} - (1-q_0)R_D \log\frac{P-e}{e} - q_V R_V \log\frac{e}{e_0} + q_V \frac{L_i^v}{T_0} + (q_{PW} + q_{CW})\frac{L_i^w}{T_0}$$

where $q_0$ denotes the total amount of water per kg of air; $C_P$, the total heat capacity at constant pressure of the mixture of air and water; $e$, the partial pressure of water vapor; and $e_0$, its saturation value computed at the reference temperature $T_0$.

## REFERENCES


Drofa, O.V., 2003. The parameterization of microphysical processes for atmospheric numerical models. Il Nuovo Cimento, 26, N.3, pp. 233-262.

Malguzzi, P., and N. Tartaglione, 1999: An economical second order advection scheme for numerical weather prediction. Q.J.R.Meteorol.Soc., 125, 2291-2303.

Marecal V., D. Hauser, and F. Roux, 1993. The12/13 January 1988 narrow cloud-frontal rainband observed during MFDP/FRONT 87. Part II: Microphysics. J.Atm.Sci., 50, 975-998.

Marshall J.S., and W. Palmer, 1948. The distribution of raindrops with size. J.Meteor., 5, 165-166.

Oblaka i Oblachnaja Atmosfera (Clouds and cloudy atmosphere), 1989. *Spravochnik pod red*. (Handbook edited by) Mazina I.A., A.KH. KHrgiana. L., Gidrometizdat, 648pp., in Russian.

Rutledge S.A., and P.V. Hobbs, 1983. The mesoscale and microscale structure and organisation of clouds and precipitation in midlatitude cyclones. VIII: A model for the «Seeder-Feeder» process in warm-frontal rainbands. J.Atm.Sci., 40, 1200-1206.

Srivastava P.C., and J.L. Coen, 1992. New explicit equations for the accurate calculation of the growth and evaporation of hydrometeors by the diffusion of vapour. J.Atmos.Sci., 49, 1643-1651.

Volkovitzkiy O.A. et al., 1983. Issledovanie spektral'nogo propuskaniya kristallicheskih tumanov (Study of spectrum transparency of crystal fogs). Izvestiay of Sciences Academy of USSR, 19, N.5, pp. 497-503.